JOURNAL OF CATALYSIS **161,** 704–712 (1996)
ARTICLE NO. 0232

The Catalytic Activity of Platinum-Loaded Porous Smectite-like Clay Minerals Containing Different Divalent Cations for Butane Hydrogenolysis and Ethylene Hydrogenation

M. Arai, S.-L. Guo, M. Shirai, Y. Nishiyama, and K. Torii*

*Institute for Chemical Reaction Science, Tohoku University, Katahira, Aoba-ku, Sendai 980-77, Japan; and *National Industrial Research Institute of Tohoku, Nigatake, Miyagino-ku, Sendai 983, Japan*

Received October 31, 1995; revised March 12, 1996; accepted March 25, 1996

Supported platinum catalysts were prepared using newly synthesized porous smectite-like clay minerals containing different divalent cations of Ni^{2+}, Co^{2+}, Mg^{2+}, and Zn^{2+} in trioctahedral sheets. Platinum was loaded on the clay minerals through the adsorption of metal precursors followed by the reduction with hydrogen. The activities of the catalysts prepared for *n*-butane hydrogenolysis and ethylene hydrogenation were shown to depend significantly on the support used, being in the order of Pt/SM (Ni) > Pt/SM(Co) > Pt/SM(Mg) ≫ Pt/SM(Zn), where SM(M) denotes the smectite-like clay mineral containing M^{2+} cation. The former three catalysts are much more active compared with a control Pt/SiO_2 catalyst. The Pt/SM(Zn) catalyst is inactive, probably due to a toxic effect of Zn^{2+} on platinum. The high catalytic activities observed may be explained by high degrees of platinum dispersion for Pt/SM(Co) and Pt/SM(Mg) catalysts. The highest activity of Pt/SM(Ni) catalyst may be attributable to the presence of different reactive sites more active than platinum. These active sites are reduced nickel species arising from the support, which are produced by platinum-catalyzed hydrogen reduction. © 1996 Academic Press, Inc.

INTRODUCTION

Clay minerals, natural and synthetic, are a big group of interesting catalytic materials (1, 2) since they have the variety of composition and structure, leading to various catalytic properties. Torii and Iwasaki invented a new hydrothermal method to synthesize trioctahedral smectite-like clay minerals that are intercalated with small fragments of anisotropic silicate and have high surface area (3–7). They have produced various smectite- and hectorite-like minerals including different divalent cations for Mg^{2+} in octahedral sheets. For several newly synthesized clay minerals, the present authors studied their physical properties and catalytic activities for the thermal decomposition of 2-propanol (8). It is an interesting result that the reaction products contain a series of oligomers of propene as well as condensates of acetone and propene. Those catalytic actions are attributable to the structural features of the clay minerals used.

In the present work, the authors have used those new synthetic clay minerals as supports of a metal catalyst and studied the effects of their structural and chemical features on catalytic activities. A metal, platinum, was supported on smectite-like clays including different divalent cations of Ni^{2+}, Co^{2+}, Mg^{2+}, and Zn^{2+}. The activities of the platinum catalysts prepared were examined for *n*-butane hydrogenolysis and ethylene hydrogenation, together with the characterization of their physical properties by temperature-programmed reduction and desorption, extended X-ray absorption fine structure, extraction of divalent cations, and other techniques. The striking influence of the supports on the catalytic activities was observed and it is discussed in terms of mutual interactions of platinum and support depending significantly on the kind of smectite-like clay minerals.

EXPERIMENTAL

Sample Preparation

Porous smectite-like clay samples were prepared by a method similar to that used previously (3–8). A Si–M (M, divalent metal) solution was prepared by dissolving metal salt in an acidic silicate solution and sodium hydroxide was added to this solution, producing a precipitate of Si–M hydroxide. The precipitate was filtered and washed with distilled water. The Si–M slurry obtained was treated hydrothermally in an autoclave at 473 K under autogaseous water vapor for 2 h. Then, the resultant mixed oxide was dried at 353 K and ground in a mortar to 32–60 mesh size.

In addition to those powdered smectite-like clay materials, a silica gel was also used as a control support. The properties of the support materials used are given in Table 1. Two smectite-like clay samples including Ni^{2+} or Co^{2+} were prepared by using different pH values of the hydrothermal treatment.

Platinum was loaded by adding a weighed quantity of the support powder to the desired volume of tetraammine-

0021-9517/96 $18.00

TABLE 1

Smectitic Clay Minerals and Silica Gel Used as Supports

Symbol	pH[a]	Composition[b] Si	M	Na	Methylene blue adsorbed (meq/g)	Specific surface area[c] (m^2/g)	Total pore volume[c] (ml/g)	Average pore diameter[c] (nm)
SM(Ni)	6.0	8	5.75	0.14	0.20	429	0.38	3.6
SM′(Ni)	11.7	8	6.16	1.86	0.68	359	0.21	2.4
SM(Co)	6.1	8	5.98	0.22	0.14	380	0.34	3.6
SM′ (Co)	9.0	8	6.34	0.85	0.68	202	0.16	3.2
SM(Mg)	9.3	8	6.13	0.38	0.28	485	0.40	3.3
SM(Zn)	6.6	8	6.53	1.28	0.24	153	0.17	4.3
SiO_2 [d]						300[e]	1.15[e]	

[a] pH for hydrothermal synthesis of smectitic clays.
[b] Number of atoms in the unit cell measured by an X-ray fluorescence method. M: Ni, Co, Mg, or Zn.
[c] Determined from nitrogen adsorption isotherms.
[d] Silica gel, Davisil grade 646 of Aldrich Chemical Company.
[e] From Aldrich's catalog handbook.

platinum dichloride solution of 20 mmol/liter. The pH was adjusted to 11 by adding ammonia solution and the support was kept immersed in this solution at room temperature for 3 days. Under the conditions used, almost all of the platinum precursors present in the solution were adsorbed by the support. After filtration, the powder was washed with distilled water and vacuum dried at 383 K for 3 h. The quantity of platinum loaded was fixed mainly to 1 wt%. The actual amounts of platinum loaded were examined by measuring the residual amounts of the metal remaining in the solution by atomic absorption spectrometry (AAS). The actual weights loaded were in good agreement with the nominal value. The platinum-loaded samples were reduced by flowing hydrogen at 96 ml/min at 573–773 K, chiefly at 673 K.

In addition, 5 wt% nickel-loaded silica gel catalyst was also prepared by a method of impregnation (9), as a reference to SM(Ni). The silica gel powder was immersed in an aqueous solution of nickel nitrate, and the solvent was removed by evaporation at about 330 K under reduced pressure. The nickel-loaded sample obtained was vacuum dried at 373 K and reduced by hydrogen at 673 K.

Activity Measurement

The activities of the catalysts prepared were tested for structure-sensitive and -insensitive reactions, *n*-butane hydrogenolysis and ethylene hydrogenation.

Hydrogenolysis of *n*-butane was performed in a fixed-bed flow-type reactor made of quartz tube of 7 mm I.D. A catalyst sample, normally 0.20 g, was reduced in the reactor by flowing hydrogen. Then, the reaction was conducted by passing the mixture of *n*-butane and hydrogen of 1 : 6 in volume at 35 ml/min over the sample at atmospheric pressure and at a temperature of 453–673 K. The reaction products were analyzed by a gas chromatograph (GC) with a column packed with VZ-7 and a thermal conductivity detector (TCD). The VHSV was 10.5 liters $\cdot h^{-1} \cdot g^{-1}$ under standard conditions and in some rums it was changed in the range of 10.5 to 2.5 liters $\cdot h^{-1} \cdot g^{-1}$ with the constant ratio of *n*-butane to hydrogen to control the conversion (Fig. 2).

Hydrogenation of ethylene was also performed at a temperature of 273 K using a similar flow-type tube reactor. A reaction mixture of ethylene and hydrogen of 1 : 1.8 in volume was passed at 55 ml/min over a catalyst of 10 mg reduced at 673 K, the VHSV being 330 liters $\cdot h^{-1} \cdot g^{-1}$. The reaction products were analyzed by a GC with an activated carbon column and TCD.

Temperature-Programmed Reduction and Desorption (TPR and TPD)

TPR and TPD were conducted with similar apparatus and procedures to those used previously (10, 11). For TPR, a sample of 0.15 g was treated at 423 K under dynamic evacuation for 1 h. After cooling to room temperature, the mixture of hydrogen and argon of 1 : 19 in volume was passed through the sample at 50 ml/min and the sample temperature was raised at 10 K/min. A TCD was used to detect the relative amount of hydrogen consumed. A column packed with molecular sieves 5A was set up between reactor and TCD and it was cooled by cold methanol at <250 K to trap species like water that would evolve during TPR and disturb the measurement of hydrogen consumed. For TPD of hydrogen, a sample of 0.15 g was exposed to hydrogen stream at room temperature for 20 min and then it was heated at 30 K/min up to 673 K while passing argon as a carrier at 30 ml/min. The amount of desorbing hydrogen was detected by TCD.

Extended X-Ray Absorption Fine Structure (EXAFS)

The EXAFS experiments were performed to examine the structure of a selected smectite-like clay mineral of SM(Ni) and metal particles dispersed on it at BL-7C and BL-10B stations of Photon Factory of National Laboratory

for High Energy Physics (Proposal 94G204). For metal particles on SM(Ni), we used a sample of Pd/SM(Ni) instead of Pt/SM(Ni). The support, SM(Ni), includes a large quantity of nickel as shown in Table 1, so the nickel K-edge absorption is very strong in a similar energy range to the platinum K-edge absorption. It was thus impossible to measure the K-edge absorption by platinum with transmission mode. The Pd/SM(Ni) sample was prepared in the same way as Pt/SM(Ni). The SM(Ni) and Pd/SM(Ni) samples were examined in the forms of pressed thin wafer and powder as it was, respectively. The samples were treated in a quartz cell by a mixture of 16% hydrogen in helium at different temperatures for 1 h. The cell was evacuated and cooled, and then the EXAFS measurement was performed at room temperature. For SM(Ni) and Pd/SM(Ni), nickel and palladium K-edge absorption spectra were collected, respectively. EXAFS oscillations were extracted from the raw data using a cubic spline method and normalized with the edge height. The k^3-weighted spectra were Fourier transformed to R space over the range of 25 to 135 nm^{-1}. The inversely Fourier fitting data were analyzed by a curve fitting method (12). The phase shifts and backscattering amplitude for nickel–nickel and palladium–palladium were determined from EXAFS data measured for nickel and palladium foils, respectively.

Extraction by Nitric Acid and Dimethylglyoxime (DMGO)

To examine the state of M^{2+} in the smectite-like clay minerals, selected samples were subjected to treatments with nitric acid and DMGO solution. Samples of 0.3 g of platinum-loaded and unloaded SM(Ni) were added to 100 ml of 6 wt% nitric acid solution of initial pH ~1. The samples were kept immersed in the solution at room temperature for 2 weeks. Then, the amount of nickel extracted in the solution was measured by AAS. Samples of 0.05 g of the smectite-like clay, SM(Ni) and SM(Co), were immersed in 15 ml of ethanol solution of DMGO of 0.3 wt% at pH ~9 at room temperature for 4 days, followed by filtration, washing with ethanol, and vacuum drying at 383 K. The treated and untreated samples were examined by scanning electron microscopy with X-ray probe microanalysis (SEM-XMA, Hitachi S-530S, Horiba EMAX-1700) to compare the composition of their surface layers.

Other Characterizations

The surface and bulk properties of selected catalyst samples were examined by X-ray photoelectron spectroscopy (XPS, Shimadzu ESCA-750), transmission electron microscopy (TEM, Hitachi H-300), and X-ray diffraction (XRD, Shimadzu XD-D1w). The samples were subjected to these measurements after they were ground in a mortar to powder. For XPS, the sample powder was mounted on a sample holder, introduced into an analysis chamber, and sputtered with Ar^+ ions. The Pt4*d* spectrum was measured with a resolution of 0.1 eV and the binding energy was charge-referenced to C1*s* binding energy of 285 eV (13). For TEM, the sample powder was well dispersed in methanol by the use of ultrasound. A few drops of the suspension were added to a carbon-coated TEM grid and dried in air. The samples were examined with a minimum detectable particle size of around 1 nm. For XRD, the sample powder was pressed into a holder and the XRD pattern was measured by using CuK_α (for SM(Ni) samples) and FeK_α (for SM(Co) samples) X rays.

RESULTS AND DISCUSSION

Catalytic Activity in n-Butane Hydrogenolysis

It was observed that the catalytic activity decreased with the time of reaction and the rate of deactivation depended on reaction temperature used. For Pt/SM(Co) catalyst, for example, the activity loss in the initial 60 min was 8% at 503 K and 23% at 533 K. The initial activities will be hereafter presented to compare the catalytic performance. It was found, however, that the selectivity changed only slightly during the reaction. The reaction products were methane (C_1), ethane (C_2), propane (C_3), and isobutane (i-C_4).

Figure 1 gives the total conversion of *n*-butane as a function of reaction temperature for platinum-loaded catalysts reduced at 673 K, showing large differences in the catalytic activities. There is no difference in the activity between Pt/SM(Ni) and Pt/SM′(Ni) catalysts in spite of the difference between the supports in some physical properties shown in Table 1. This is also the case for Pt/SM(Co) and Pt/SM′(Co) catalysts. The catalysts using the smectite-like clay minerals except SM(Zn) indicate

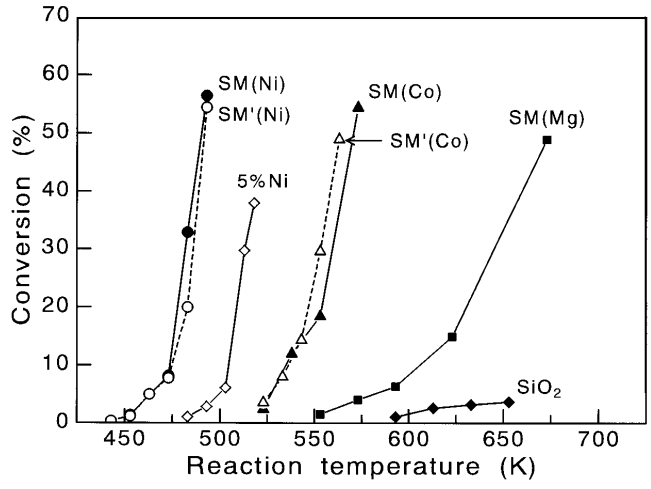

FIG. 1. The catalytic activity for *n*-butane hydrogenolysis as a function of reaction temperature for 1 wt% platinum-loaded catalysts using five different smectite-like clay minerals and silica gel and 5 wt% nickel-loaded silica gel catalyst.

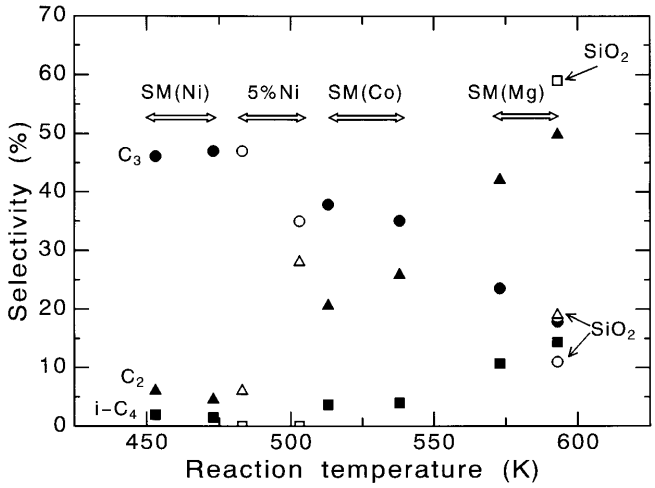

FIG. 2. The selectivities in *n*-butane hydrogenolysis as a function of reaction temperature for 1 wt% platinum and 5 wt% nickel catalysts. Closed marks indicate the results measured at a total conversion of 10% for platinum-loaded SM(Ni), SM(Co), and SM(Mg) catalysts. Open marks show the results for Pt/SiO_2 and Ni/SiO_2 catalysts, the conversion being 1% (593 K) for the former and 1% (483 K) and 6% (503 K) for the latter. Circles, triangles, and squares are the selectivities to C_3, C_2, and i-C_4, respectively. The selectivity to C_1 is the same as that to C_3.

much higher activities compared with Pt/SiO_2, being in the order of Pt/SM(Ni) > Pt/SM(Co) > Pt/SM(Mg). In contrast, the Pt/SM(Zn) catalyst was found to be inactive at temperatures up to 673 K. When SM(Ni) and SM(Co) were reduced at 673 K in the absence of platinum, they were inactive at reaction temperatures examined. Figure 1 also includes the result of 5 wt% nickel-loaded silica catalyst, which is highly active compared with 1% Pt/SiO_2. Platinum is less active than nickel and cobalt in some hydrogenolysis reactions, according to Sinfelt (14), van Broekhoven and Ponec (15), and Garin *et al.* (16).

Figure 2 shows the selectivity at a total conversion of 10% as a function of reaction temperature for platinum-loaded SM(Ni), SM(Co), and SM(Mg) catalysts. The Pt/SM(Ni) catalysts produces C_3 more selectively compared with C_2 and i-C_4. With going through Pt/SM(Co) to Pt/SM(Mg), the selectivity to C_3 decreases while those to C_2 and i-C_4 increase.

The selectivities of those platinum-loaded smectite-like clay catalysts are significantly different from that of Pt/SiO_2 catalyst. Figure 2 also gives the selectivity of Pt/SiO_2 at 593 K and at 1% conversion, indicating a higher selectivity to i-C_4. Namely, the Pt/SiO_2 catalyst catalyzes the isomerization as well as the hydrogenolysis. In contrast, 5% Ni/SiO_2 catalyst is active only to the hydrogenolysis, as shown in Fig. 2 giving the selectivities at 483 K and 1% conversion and at 503 K and 6% conversion. Thus, it follows that the active catalysts, Pt/SM(Ni) and Pt/SM(Co), are similar to Ni/SiO_2 rather than Pt/SiO_2 with respect to the product distribution as well as the high catalytic activity.

TABLE 2

Influence of Reduction Temperature on the Activity[a] of 1 wt% Platinum-Loaded SM(Ni) Catalyst

Temperature (K)	573	623	673	723	773
Conversion (%)	3	12	33	55	100
Selectivity (%)					
C_3	48	46	43	40	41
C_2	3	7	12	19	18
i-C_4	1	1	2	1	0

[a] For *n*-butane hydrogenolysis at 483 K.

For Pt/SM(Ni), the influence of reduction temperature on the catalytic activity was examined. Table 2 presents the total conversion and selectivity after reduction at temperatures of 573 to 773 K. The activity increases with increasing reduction temperature. The catalyst is still highly active even after the reduction at 773 K that probably causes the growth of dispersed platinum particles as indicated by EXAFS data. The selectivity to a main product, C_3, slightly decreases with increasing temperature (increasing conversion), while the selectivity to C_2 increases.

The presence of platinum is indispensable for the smectite-like clay minerals to take high catalytic activities even though it is not so active species. To examine the role of platinum, we attempted to load 1 wt% platinum to 5% Ni/SiO_2, a reference to SM(Ni). The platinum was added to a reduced Ni/SiO_2 sample by an impregnation method similar to that used in the preparation of Ni/SiO_2. In addition, platinum was also added to an unreduced Ni/SiO_2 sample by the same adsorption method as used in the loading to the smectite-like clays. Figure 3 gives the catalytic activities of those samples, denoted with a and b, respectively, after

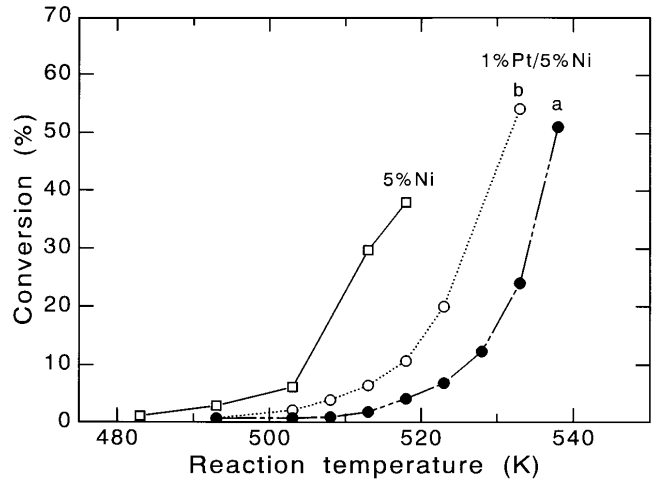

FIG. 3. The influence of the doping of platinum in 1 wt% on the activity of a 5 wt% nickel-loaded silica gel catalyst for *n*-butane hydrogenolysis. The two platinum-doped catalysts a and b given are different in the way of platinum doping as described in the text.

TABLE 3

Activity of 1 wt% Platinum-Loaded Catalysts Reduced at 673 K for Ethylene Hydrogenation at 273 K

Support	SM(Ni)	SM(Co)	SM(Mg)	SiO_2	SM(Zn)
Activity[a]	59.4	59.1	49.7	5.4	Inactive

[a] In $mmol \cdot min^{-1} \cdot g_{cat}^{-1}$.

reduction at 673 K, showing negative effects that the loading of platinum decreases the activity of the Ni/SiO_2 catalyst. It seems that the platinum in the smectite-like clays plays different roles compared with the platinum on Ni/SiO_2.

Catalytic Activity in Ethylene Hydrogenation

Table 3 presents the activities of platinum-loaded catalysts reduced at 673 K. They were not found to indicate deactivation during the activity measurement for 60 min. The activity strongly depends on the support used, being in the same order of $Pt/SM(Ni) \approx Pt/SM(Co) > Pt/SM(Mg) > Pt/SiO_2$ as in *n*-butane hydrogenolysis. Again, Pt/SM(Zn) catalyst was inactive; it only had a low activity of 0.4 $mmol \cdot min^{-1} \cdot g_{cat}^{-1}$ at a higher reaction temperature of 373 K.

TPR and TPD

Figure 4 shows TPR spectra for the samples of platinum on smectite-like clays and silica. The Pt/SiO_2 sample has a peak maximum at around 400 K ascribable to the reduction of platinum precursors. The other samples show peaks at higher temperatures depending on the smectite-like clay mineral used. This indicates that higher temperatures are required to reduce the platinum precursors dispersed in the clays. For the catalytically active samples, Pt/SM(Ni) and Pt/SM(Co), the platinum was able to reduce at lower

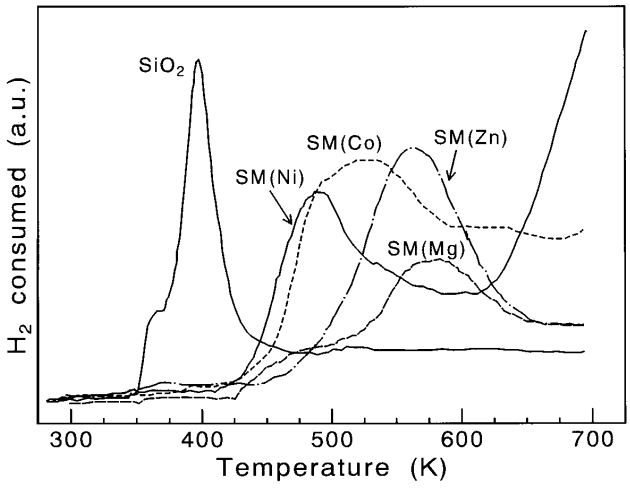

FIG. 4. The TPR profiles for 1 wt% platinum-loaded smectite-like clay and silica gel samples.

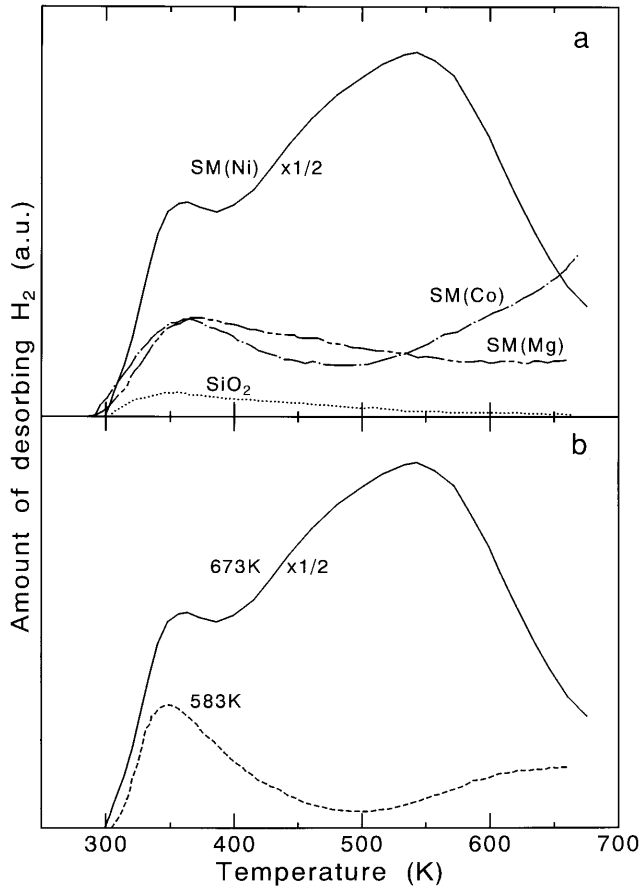

FIG. 5. TPD spectra of hydrogen for 1 wt% platinum-loaded catalysts on different supports after reduction at 673 K (a) and for 1 wt% Pt/SM(Ni) catalyst reduced at 673 and 583 K (b).

temperatures and excess amounts of hydrogen were consumed at higher temperatures above 650 K. This suggests that hydrogen was adsorbed on the samples and/or it was also used to reduce some other species like M^{2+} present. It can be said that for all the samples examined, the dispersed platinum precursors are reduced by the standard reduction at 673 K of the catalyst preparation.

The TPD spectra of hydrogen for 1 wt% platinum-loaded catalysts reduced at 673 K are shown in Fig. 5a, indicating marked differences between them. Table 4 presents the total amounts of hydrogen desorbing during the TPD up to 673 K. Excess hydrogen is adsorbed by the catalysts using the smectite-like clays, particularly Pt/SM(Ni); in

TABLE 4

Results of TPD of Hydrogen for 1 wt% Platinum-Loaded Catalysts Reduced at 673 K

Support	SM(Ni)	SM(Co)	SM(Mg)	SiO_2	SM(Zn)
Uptake (H/Pt)	8.69	1.42	1.23	0.19	0.06

other words, large quantities of hydrogen spillover from the platinum to the support for these catalysts. Figure 5b shows the influence of reduction temperature on the TPD for Pt/SM(Ni). This catalyst adsorbed less hydrogen and indicated a similar spectrum to Pt/SM(Co) catalyst reduced at 673 K when it was reduced at a lower temperature of 583 K (the second large consumption of hydrogen began at a little higher temperature on the TPR as seen in Fig. 4). That is, the Pt/SM(Ni) catalyst becomes greatly different from the other catalysts when the reduction temperature is raised to 673 K. In contrast, the amount of hydrogen adsorbed was very small for Pt/SM(Zn) catalyst. A degree of metal dispersion of 0.06 gives an estimate of average particle size of 17 nm (17). However, TEM failed to detect such large platinum particles on Pt/SM(Zn). So, its small hydrogen uptake was due to factors other than the size of platinum particles present.

EXAFS

EXAFS was used to examine the structure of a smectite-like clay mineral of SM(Ni). Figure 6 shows Fourier transforms of nickel K-edge EXAFS oscillations for platinum-loaded and unloaded SM(Ni) samples with respect to the local structures around nickel species. The SM(Ni) and Pt/SM(Ni) reduced at 673 K indicate very similar results that the first and second nearest species, oxygen and nickel, are present at 0.205 and 0.308 nm, respectively. This indicates that the structure of SM(Ni) did not change by the loading of platinum and the subsequent reduction at 673 K. This was also shown by XRD measurements. On the reduction at a higher temperature of 773 K, a small peak appeared at 0.250 nm. The curve-fitting analysis showed that the oscillation derived from nickel–nickel bond fitted well the inversely Fourier transform of the peak. This indicates the formation of direct bonds between nickel atoms.

The structure of metal particles dispersed on SM(Ni) was examined by using a Pd/SM(Ni) sample instead of Pt/SM(Ni). Figure 7 gives Fourier transforms of palladium K-edge EXAFS oscillations for palladium-loaded catalysts reduced at 673 and 773 K. A peak present at 0.261 nm was fitted well to palladium–palladium bond and its intensity is stronger at higher reduction temperature. To get the best result for the curve-fitting analysis, four free parameters were estimated: the coordination number, the bond length, the Debye–Waller factor, and the inner potential correction. The coordination number was estimated to be 4.2 and 7.7 at 673 and 773 K, respectively, indicating that the size of dispersed palladium particles is larger at higher temperature. Probably, this is the case for Pt/SM(Ni) samples as well.

In addition, palladium in a Pd/SM(Co) catalyst was examined by EXAFS. The coordination number was estimated to be 5.2 for the catalyst reduced at 673 K, and it is comparable to that for Pd/SM(Ni). This indicates that there is little difference in the size of metal particles between SM(Ni) and SM(Co) supports.

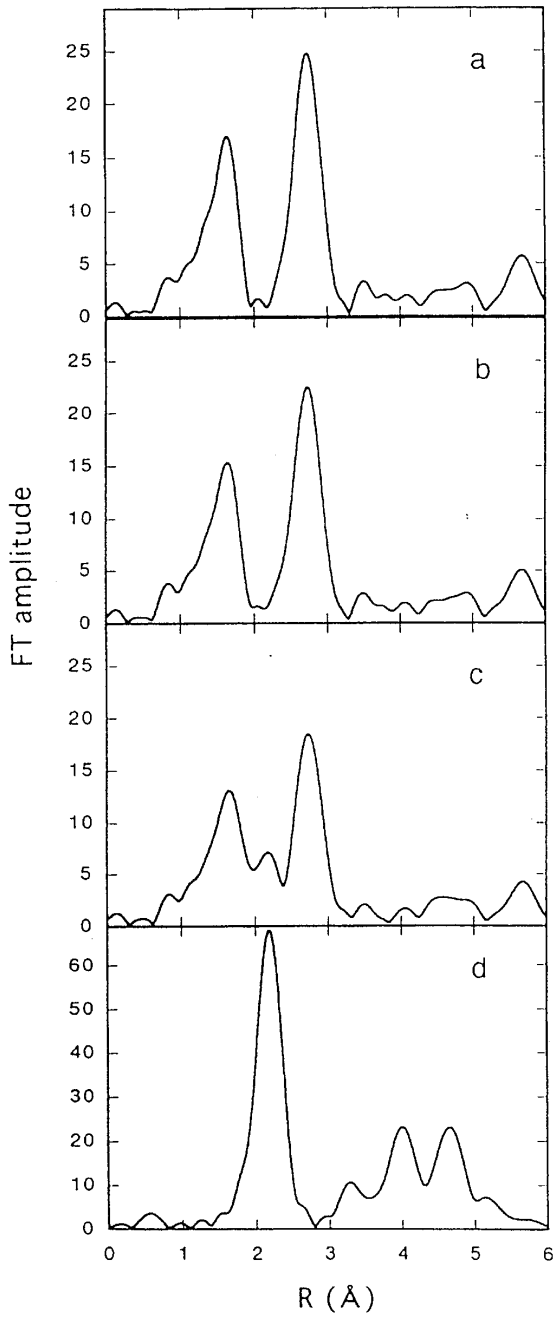

FIG. 6. Fourier tramsfroms of the k^3-weighted Ni K-edge EXAFS of SM(Ni) (a), 1% Pt/SM(Ni) catalysts reduced at 673 K (b) and 773 K (c), and a nickel foil (d).

Figure 7 indicates a support effect that the length of palladium–palladium bond of Pd/SM(Ni) is shorter than that of a palladium foil, probably due to smaller sizes of palladium particles in Pd/SM(Ni). A few works reported that the first coordination distance of metal–metal bonds for small metal particles in supported catalysts is smaller

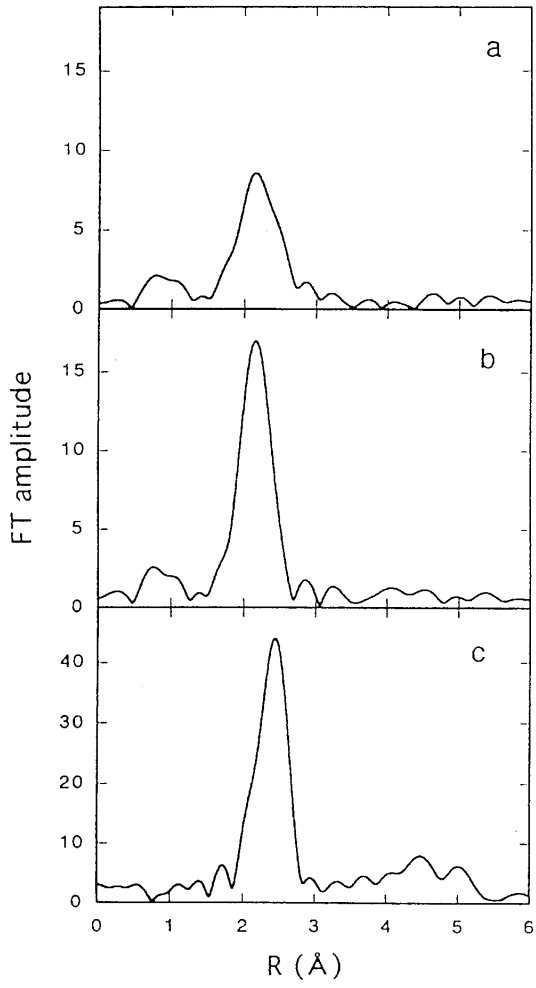

FIG. 7. Fourier transfroms of the k^3-weighted Pd K-edge EXAFS of 1% Pd/SM(Ni) catalysts reduced at 673 K (a) and 773 K (b), and a palladium foil (c).

compared with that in bulk metal samples when EXAFS measurements were conducted under vacuum conditions (18–20).

Extraction by Nitric Acid and DMGO

Table 5 gives the amounts of nickel extracted from SM(Ni) and Pt/SM(Ni) samples by the treatment with nitric acid for 2 weeks. The amount of nickel extracted is about 30% of the initial quantity of nickel present in the clay, being about 10% relative to the total weight of the whole samples.

Table 6 presents results of the treatment of SM(Ni) and SM(Co) by DMGO. The XMA intensity ratio of Ni (or Co) to Si was found to decrease by the treatment, indicating that Ni and Co species were also extracted by DMGO. The extracted amounts are smaller than those by nitric acid, due to a difference in the extracting ability between DMGO and the acid.

TABLE 5

Results of Acid Extraction of Nickel from SM(Ni) and 1 wt% Platinum-Loaded SM(Ni) Samples

Sample	Amount of nickel extracted in weight percent[a]	
	To the whole	To the nickel
SM(Ni), original	12	33
SM(Ni), reduced[b]	12	31
Pt/SM(Ni), reduced[b]	10	27

[a] Relative to the initial amount of the whole sample and the nickel included.
[b] At 673 K.

Those results suggest that Ni and Co species in the SM (Ni) and SM(Co) may take positions at the surface and become accessible to foreign species by appropriate treatments.

In addition, we examined the influence of the extraction of SM(Ni) by nitric acid prior to the loading of platinum on the catalytic activity. Figure 8 compares the activities for *n*-butane hydrogenolysis. The catalysts using SM(Ni) supports treated by nitric acid also have high activities. The acid treatments for 3 and 24 h caused the weight loss of SM(Ni) by 4 and 17%, respectively, relative to the initial weight.

Origin of the Catalytic Activity

The present results demonstrate that the catalysts of platinum-loaded smectite-like clay minerals, except for Pt/SM(Zn), are highly active in *n*-butane hydrogenolysis and ethylene hydrogenation compared with Pt/SiO_2 catalyst. The high activities for a structure-insensitive reaction of ethylene hydrogenation may be explained by the high degrees of metal dispersion. The order of the platinum dispersion seems to be Pt/SM(Ni) ≈ Pt/SM(Co) > Pt/SM(Mg) > Pt/SiO_2 > Pt/SM(Zn) from the results of TPD and EXAFS. For the Pt/SM(Zn) catalyst, its activity could be expected to be about 1/3 of the Pt/SiO_2 catalyst

TABLE 6

Results of Extraction of M^{2+} from SM(Ni) and SM(Co) by DMGO as Examined by SEM-XMA

Sample	$I(M^{2+})/I(Si)$[a]		
SM(Ni)			
Before	0.97	0.97	0.97
After	0.89	0.93	0.87
SM(Co)			
Before	1.3	1.3	1.2
After	1.1	1.1	1.0

[a] XMA intensity ratios measured at three different positions before and after the extraction.

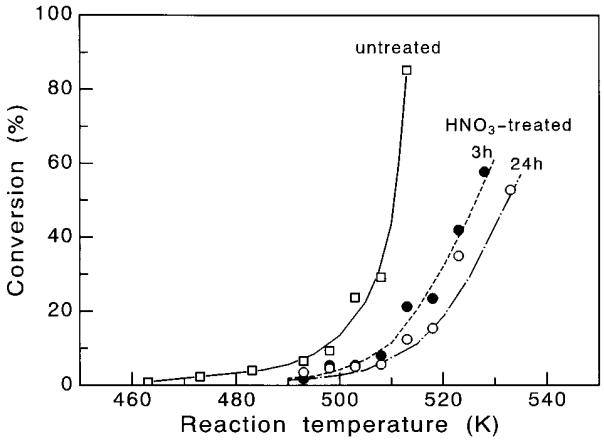

FIG. 8. The influence of the treatment of SM(Ni) with nitric acid for 3 and 24 h on the activity of a 0.1 wt% platinum-loaded SM(Ni) catalyst for *n*-butane hydrogenolysis. The treatment was made prior to the loading of platinum to SM(Ni).

from the degrees of platinum dispersion (Table 4). However, it is actually inactive, so another explanation should be offered. A possible reason is the influence of Zn^{2+} present in the support. It is known that Zn^{2+} is a poison toward platinum as described by Maxted (21). We tried to dope a small amount of zinc species to a reduced Pt/SiO_2 catalyst and examined its influence on the catalytic activity. The amount of zinc corresponding to a coverage of 0.85 of the whole surface of platinum particles was doped by impregnation from zinc nitrate solution followed by reduction at 673 K. Negative effects were observed for both ethylene hydrogenation and *n*-butane hydrogenolysis, the activity being decreased by factors of 1/4 and 1/7.5, respectively. Thus, the zinc species inhibit the activity of platinum supported on SM(Zn).

The activities of the catalysts, except for the most active Pt/SM(Ni) and inactive Pt/SM(Zn), for *n*-butane hydrogenolysis may be explained by the size of platinum particles. The hydrogenolysis is a structure-sensitive reaction and so the degree of platinum dispersion would have more significant effects on it than on a structure-insensitive reaction of ethylene hydrogenation. Table 7 shows the apparent activation energy, the rate of reaction (the rate of consumption of *n*-butane molecules), and turnover frequency (TOF) for five different catalysts except for Pt/SM(Zn). The numbers of active sites were determined by the TPD of hydrogen (Table 4) for the calculation of TOF. Significant support effects can be seen from Table 7. It should be noted that the Pt/SM(Ni) is more similar to Ni/SiO_2 than to the catalysts using the other smectite-like clay minerals. The high catalytic activity of Pt/SM(Ni) cannot be expected from its degree of platinum dispersion comparable to that of Pt/SM(Co) catalyst. It still has the high activity after the reduction at 773 K that causes the growth of platinum particles. In addition, the Pt/SM(Ni) catalyst gives the product distribution that is similar to Ni/SiO_2 catalyst rather than Pt/SiO_2 catalyst; namely, it mainly produces C_3 than C_2 and i-C_4.

From those results, we assume that the Pt/SM(Ni) catalyst includes other reactive sites more active than platinum, and nickel species of the support can become such active sites. They are supposed to form in such a way that the platinum precursors are reduced to metallic platinum in the early stage of reduction and the resultant platinum catalyzes the formation of active nickel sites in the following stage. The large amount of hydrogen consumed at a high temperatures during TPR should indicate the formation of those species. The excess uptake of hydrogen should indicate the presence of reduced nickel sites, as well as platinum, on the surface of the Pt/SM(Ni) catalyst. The higher reduction temperature is likely to promote the formation of the nickel species, resulting in an increase in the catalytic activity as shown in Table 2. The nickel species may be main active sites for *n*-butane hydrogenolysis than the platinum. Previously

TABLE 7

Comparison of Catalytic Activities for *n*-Butane Hydrogenolysis

Catalyst[a]	Apparent activation energy[b] ($kJ \cdot mol^{-1}$)		530 K		500 K	
			Rate[b] ($mol \cdot min^{-1} \cdot g^{-1}$)	TOF[b] (min^{-1})	Rate[b] ($mol \cdot min^{-1} \cdot g^{-1}$)	TOF[b] (min^{-1})
Pt/SM(Ni)	178	(453–493 K)[c]	1.34×10^{-2}	30.0	1.19×10^{-3}	2.67
Pt/SM(Co)	146	(523–573 K)[c]	5.16×10^{-5}	0.71	7.09×10^{-6}	0.097
Pt/SM(Mg)	86	(553–673 K)[c]	8.43×10^{-6}	0.13	2.62×10^{-6}	0.042
Pt/SiO_2	63	(593–653 K)[c]	3.05×10^{-6}	0.31	1.30×10^{-6}	0.133
Ni/SiO_2	221	(483–518 K)[c]	1.29×10^{-3}	22.3	6.36×10^{-5}	1.10

[a] The amounts of metal loaded are 1 and 5 wt% for Pt and Ni catalysts, respectively. For 5% Ni/SiO_2 sample, the degree of metal dispersion was determined to be 0.068 by the TPD of hydrogen measured under the same conditions as for the Pt catalysts. The Pt/SM(Zn) catalyst is inactive at temperatures below 673 K.

[b] For some catalysts, rate and TOF were estimated by extrapolation to those reaction temperatures.

[c] The activation energy was determined from the data measured in the range of reaction temperature given in parentheses.

Nowak and Koros reported a similar effect of platinum on the activation of an alumina-supported nickel catalyst; a small amount of platinum added catalyzed hydrogen reduction of supported nickel oxide following the early reduction of platinum itself (22). For supported nickel-platinum catalysts, Renouprez *et al.* showed synergistic effect attributable to modifications of the electronic properties of both metals (23). In our Pt/SM(Ni) catalyst, no evidence was obtained for direct bonds and electronic interactions between platinum and nickel from EXAFS and XPS measurements.

The formation of active nickel sites accessible to foreign gases in Pt/SM(Ni) catalyst would have occurred through a structural change of surface layer of the support. Surface nickel species are likely to come out from the two sources, smectite-like silicate layers and small silicate fragments intercalated as pillars. Nickel cations may move to the top surface positions from the inner positions of those silicate layers and fragments. The occurrence of such a movement of the nickel is strongly suggested by the results on the extraction of SM(Ni) with nitric acid and DMGO. After moving to the top surface, nickel species may be reduced to the metallic state having catalytic activities. These structural and chemical changes may be facilitated by the action of metallic platinum, supplying reactive hydrogen species to the peripheral surface of support close to platinum particles. It was previously reported that metal ions depleted from the octahedral sheets of clay minerals by acid hydrolysis (24). A proposed mechanism for this depletion involves proton attack at the edges of the layers for nonswelling clays (25). The other mechanism is also presented, involving proton attack at the basal surfaces for swelling clays (26) like the smectite-like clay minerals used in the present work. For out Pt/SM(Ni) sample, active hydrogen species that form on the metallic platinum particles spillover onto the support and would cause the structural change, similarly to protons in the acid hydrolysis. The excess hydrogen uptake of H/Pt = 8.69 (Table 4) indicates that the quantity of exposed nickel atoms is only a few per cent of those present in the SM(Ni). So, the structural change is likely to occur at the edges of the smectitic silicate layers and intercalated silicate fragments.

CONCLUSIONS

The samples of platinum supported on new synthetic smectite-like clay minerals of SM(Ni), SM(Co), and SM(Mg) are highly active catalysts for *n*-butane hydrogenolysis and ethylene hydrogenation compared with silica-supported platinum catalyst, while the Pt/SM(Zn) sample is an inactive catalyst. The most active catalyst, Pt/SM(Ni), is strikingly different from the other catalysts in that its high activity is a result of mutual interactions between platinum and support. This catalyst includes reactive nickel sites, more active than platinum, that come out from the support by platinum-catalyzed hydrogen reduction. The high activities of Pt/SM(Co) and Pt/SM(Mg) are attributable to enhanced degrees of platinum dispersion and little activity of Pt/SM(Zn) is due to a toxic effect of Zn^{2+}.

ACKNOWLEDGMENT

The authors are grateful to G. Fukatani for his help in the preparation of platinum catalyst samples.

REFERENCES

1. Anderson, J. R., "Structure of Metallic Catalysts," p. 74. Academic Press, New York, 1975.
2. Satterfield, C. N., "Heterogeneous Catalysis in Practice," p. 244. McGraw–Hill, New York, 1980.
3. Torii, K., and Iwasaki, T., *Chem. Lett.* 2021 (1986).
4. Torii, K., and Iwasaki, T., *Clay. Sci.* **7**, 1 (1987).
5. Torii, K., and Iwasaki, T., *Chem. Lett.* 2045 (1988).
6. Torii, K., Iwasaki, T., Onodera, Y., and Shimada, M., *J. Ceram. Soc. Jpn. Int. Ed.* **97**, 158 (1989).
7. Torii, K., Iwasaki, T., Onodera, Y., and Shimada, M., *Nippon Kagaku Kaishi* 345 (1989).
8. Nishiyama, Y., Arai, M., Guo, S.-L., Sonehara, N., Naito, T., and Torii, K., *Appl. Catal.* **95**, 171 (1993).
9. Arai, M., Guo, S.-L., and Nishiyama, Y., *J. Catal.* **135**, 638 (1992).
10. Arai, M., Suzuki, K., and Nishiyama, Y., *Bull. Chem. Soc. Jpn.* **66**, 40 (1993).
11. Arai, M., Nishiyama, Y., Masuda, T., and Hashimoto, K., *Appl. Surf. Sci.* **89**, 11 (1995).
12. Yokoyama, T., Hamamatsu, H., and Ohta, T., Program "EXAFSH Ver. 2.1." The University of Tokyo, Tokyo, 1994.
13. Wagner, C. D., Riggs, W. M., Davis, L. E., Moulder, J. F., and Muilberg, G. E., "Handbook of X-Ray Photoelectron Spectroscopy." Perkin–Elmer Corp., Eden Prairie, MN, 1978.
14. Sinfelt, J. H., *Catal. Rev.* **3**, 175 (1969).
15. van Broekhoven, E. H., and Ponec, V., *Prog. Surf. Sci.* **19**, 351 (1985).
16. Garin, F., Hilaire, L., and Maire, G., *Stud. Surf. Sci. Catal.* **27**, 145 (1986).
17. Boudart, M., and Djega-Mariadassou, G., "Kinetics of Heterogeneous Catalytic Reactions," p. 26. Princeton Univ. Press, Princeton, 1984.
18. Gordon, M. B., Cyrot-Lackmann, F., and Desjonqueres, M. C., *Surf. Sci.* **80**, 159 (1979).
19. Moraweck, B., Clugnet, G., and Renouprez, A. J., *Surf. Sci.* **81**, L631 (1979).
20. Kampers, F. W. H., and Koningsberger, D. C., *Faraday Discuss. Chem. Soc.* **89**, 137 (1990).
21. Maxted, E. B., *Adv. Catal.* **3**, 129 (1951).
22. Nowak, E. J., and Koros, R. M., *J. Catal.* **7**, 50 (1967).
23. Renouprez, A. J., Moraweck, B., Imelik, B., Dominquez-Esquivel, J. M., and Jablonski, J., *in* "Proceedings, 7th International Congress on Catalysis, Tokyo, 1980" (T. Seiyama and K. Tanabe, Eds.), Part A, p. 173. Elsevier, Amsterdam, 1981.
24. Kaviratna, H., and Pinnavaia, T. J., *Clays Clay Miner.* **42**, 717 (1994).
25. Cetisli, H., and Gedikbey, T., *Clay Miner.* **25**, 207 (1990).
26. Rice, N. M., and Strong, L. W., *Can. Metall. Quart.* **B13**, 485 (1974).